

An Unusual Technique for the Study of Nonstoichiometry: The Thermal Emission of Electrons. Results for Y_2O_3 and TiO_2

PHILIPPE ODIER*

Centre National de la Recherche Scientifique, Centre de Recherche sur la Physique des Hautes Températures, 1D, avenue de la recherche scientifique, 45045 Orléans Cedex, France

AND JEAN-PIERRE LOUP

Laboratoire de Physique des Matériaux Solides, Faculté des Sciences, Parc de Grandmont, 37200 Tours, France

Received May 23, 1979; in revised form August 6, 1979

The thermal emission of electrons is presented as a useful technique for the study of nonstoichiometric oxides at high temperature. Results are reported for yttria and titanium dioxide, very different in their respective properties. For these compounds the density of emitted current follows a simple law, $J \propto P_{O_2}^x$, where P_{O_2} is the oxygen partial pressure and x is a constant that is not dependent on temperature. The electrical conductivity, when measured under the same conditions, follows a similar law. Therefore there is some evidence that at high temperature the chemisorption is not an important process, and the emission characteristics are then discussed in terms of a bulk nonstoichiometry. Data are obtained for yttrium oxide, as the width of the band gap $E_g = 5.5$ eV, the electron affinity $\chi = 2$ eV. A reasonable defect for this oxide consists of oxygen vacancies V_O^{2-} and oxygen interstitials O_i^{2+} . The situation in the case of rutile is much more complicated as this oxide has a wide nonstoichiometric field with several suboxides and a nonisotropic structure. When the deviation to the stoichiometry is low the oxygen sublattice is stable and the main defects are titanium interstitials Ti_i^{3+} . When the compound is more reduced a surface reorganization then occurs which seems related to a crystallographic transformation leading to the Ti_nO_{n-1} suboxides. This technique give a lot of data on the properties of nonstoichiometric compounds in the vicinity of the surface at high temperature.

1. Introduction

The thermal emission of electrons was extensively investigated during the first part of this century with the primary aim of getting good emitters for the technology of electron tubes. A lot of work was done on oxide cathodes (1) because some of them (the alkaline earth oxides) can provide an emission high enough for technical applications. Generally the oxide was activated,

which means that it was reduced at high temperature under vacuum; then it was quenched at the operating temperature. As a matter of fact the oxide that is thus obtained is not well characterized as the oxygen partial pressure is not controlled during the activation and as the background may have an important contribution. Thus the physical system could be quite complicated and there are many basic but still unresolved questions regarding the actual mechanism of the emission of such cathodes (2).

* To whom correspondence should be addressed.

As we are dealing with oxides it seems straightforward to study the emission as a function of the oxygen partial pressure, P_{O_2} , during isothermal runs. The oxide will be homogeneous and in thermodynamical equilibrium. The first experiment in this way was carried out by Loup and Anthony (3) on zirconia. From his results it has been shown that the thermal emission of electrons, followed by the density of the emitted current J , is proportional to P_{O_2} to the power x , where x is a constant that is not dependent on temperature. This important point allows one to rule out a major effect of chemisorption on the emission of electrons at high temperature ($T > 1600$ K). Thus a model involving nonstoichiometry seems to be an appropriate frame in which to explain the results.

In this paper we report additional confirmations of this property: the constant x can be used to investigate the defect structure of the compound. Two cases will be depicted below, the first of which deals with a highly refractory oxide: Y_2O_3 . Our experiment then provides useful results to discuss the nature of point defects in this compound. The other example is the much more studied titanium–oxygen system. The wide nonstoichiometric range of titanium oxide opens the field of application of our technique. However, owing to this oxide some complications arise that are discussed.

2. Theoretical

Let us summarize first briefly several theoretical aspects that will be used later on. The density of emitted current J_0 (at zero electrical field) at the temperature T is given by the Richardson–Dushman law:

$$J_0 = A_0 T^2 (1 - \bar{r}) \exp - \frac{\Phi}{kT}, \quad (1)$$

where

$$A_0 = 4\pi m e k^2 / h^3 = 120 \text{ A cm}^{-2} \text{ K}^{-2}; m \text{ is the mass of a free electron}$$

\bar{r} = the mean thermoelectron reflectance coefficient; it will be neglected below (at least its variations with the P_{O_2})

Φ = the work function: $\Phi = \chi + (E_c - E_F)$

E_F = the energy at the Fermi level

E_c = the energy at the bottom of the conduction band

Using the Boltzmann approximation for the electron concentration in the conduction band n ,

$$\frac{n}{N_c} = \exp - \frac{E_c - E_F}{kT}, \quad (2)$$

with

$$N_c = 2 \left(\frac{2\pi m k T}{h^2} \right)^{3/2};$$

Eq. (1) can be written

$$J_0 = e \left(\frac{k}{2\pi m} \right)^{1/2} T^{1/2} n \exp - \frac{\chi}{kT}. \quad (3)$$

If the effective mass m^* of the electron in the conduction band and the variation of the work function with temperature are taken into account, then:

$$J_0 = A_0 T^2 \left(\frac{m^*}{m} \right)^{3/2} \exp - \frac{1}{k} \frac{d\Phi}{dT} \exp - \frac{\Phi_0}{kT},$$

with

$$\Phi = \Phi_0 + \frac{d\Phi}{dT} T,$$

$$N_c = 2 \left(\frac{2\pi m^* k T}{h^2} \right)^{3/2}.$$

The value of $d\Phi/dT$ is not well known; however, for metals it is (4) in the range of 10^{-4} eV K^{-1} . For semiconductors the band gap decreases with the temperature: for TiO_2 the variation (5) is $dE_i/dT \approx -9 \times 10^{-4}$ eV K^{-1} as in the case of BaO (6).

As we are concerned with the variation of nonstoichiometry versus oxygen pressure it is useful to calculate the induced variation of the electron concentration in the conduction band. In the following lines this will be done

within the frame of the point defect theory (6). It is assumed that the nonstoichiometry is small enough to be in the range of validity of this theory. The nonstoichiometry can be idealized in some cases as a departure of oxygen from a sublattice of the solid, thus leaving electron donors that are either oxygen vacancies or metal interstitials. Thus as emphasized here, the electron concentration in the conduction band is a function of the oxygen partial pressure P_{O_2} :

$$n = Bk_D P_{O_2}^{-1/x}, \quad (4)$$

where

x depends upon the defect D ,

k_D is a constant of action mass with an exponential variation upon the temperature,

B is a constant varying slowly with the temperature.

The important point to underline here is that J_0 must be proportional to P_{O_2} at the power $-1/x$ (Eqs. (3) and (4)), in contrast to the electrical conductivity:

$$\sigma_e = ne\mu_e + pe\mu_p, \quad (5)$$

where μ_e and μ_p are the electron and the electron hole mobilities.

3. Experimental

The oxygen partial pressure is achieved here by introducing pure oxygen (99.99%) in a high vacuum system through a variable leak at a very low rate. The residual atmosphere is clean: in the lower pressure limit of our apparatus, 10^{-13} – 10^{-12} atm (10^{-10} – 10^{-9} Torr), the mass spectrum essentially consists of He, H_2 , N_2 , CO, and CO_2 . In such an atmosphere the oxygen partial pressure would be very low and uncontrolled, so the lower pressure reported here is in the range of 10^{-11} – 10^{-10} atm. In this lower range of oxygen pressure the background contribution remains low and decreases very quickly as the oxygen pressure increases. Below 10^{-9} atm the oxygen partial pressure is deduced from the mass spectrum (7) and

above this value it is equal to the total pressure within the limits of accuracy. The total pressure is measured with a classical ionization gauge (iridium thoriated filaments); the gauge is turned off when the pressure is known and stable. The use of a throttling valve insulating the ionic pump from the main chamber enables one to do measurements up to the atmospheric pressure. In fact in the case of the present experiments, the higher pressure limit is restricted to the range of 10^{-6} – 10^{-5} atm in order to prevent the thermalization of the electrons on the gaseous molecules: the mean free path is high enough under these conditions. Measurements are made in a low dynamic flow and the pressure is stable as long as wanted. Obviously our experiments are made under a low total pressure in contrast to the usual experiments performed under a total pressure of 1 atm in a buffer gas mixture (8). However, the earliest experiments in nonstoichiometry were made in a vacuum system (9), but the covered range of pressure was too low and cracking of hydrocarbons might have induced some contaminations. The clean vacuum systems now available offer a simple technique to monitor the oxygen pressure; it can provide measurements in a range where the oxygen partial pressure cannot be obtained with the use of gas mixtures such as CO– CO_2 or Ar– O_2 only. However, the evaporation of the compound could be a limitation in some particular cases.

The temperature is measured with an optical pyrometer calibrated on a blackbody reference. The studied oxide, covering the metallic heating wire, is taken out in a small area for the measurement of the temperature and corrections for the optical emissivity of the sighting surfaces are made. The temperature is manually adjusted but can also be regulated with an appropriate device (photodiode or Wheatstone bridge). The actual temperature range depends on the compound tested and can be very wide. The best metal for high-temperature experiments

is iridium because of its low reactivity with oxides. With such a metal measurements were made (3) up to 1900 K for ZrO_2 and (10) 1800 K for Y_2O_3 . The case of TiO_2 will be discussed later on. The lower range of temperature is limited by the small value of the emitted current as the wide band gap oxides are generally poor emitters. Measurements have been conducted down to 1300 K.

The electron emission is measured in the central anode of a cylindrical diode as a function of the applied potential V in order to plot the Schottky curves ($\log J - V^{1/2}$) which are straight lines for a homogeneous surface (4). When this is not the case, the value of J instead of J_0 is reported at a specified potential. The potential can be either static or slowly varied (0.1 to 50 Hz) between 0 and 600 V. The same results are observed when no appreciable space charge layer is created by a too-high current density (11, 12). In these measurements the cathode is grounded; it is made with a metallic iridium wire covered by electrophoretic deposition (13) with a spectroscopically pure oxide. The sample is thus polycrystalline and impurities are in very low concentration as heating under vacuum at high temperature removes all the impurities with higher vapor pressure than the oxide involved. Before the beginning of the experiment the sample is also heated at high temperature under an oxygen pressure which burns the carbon which may be present. Experiments are always started from high oxygen pressure near the stoichiometry.

In special cases it may be useful to have an idea of the crystallographic structure of the oxide after experiments. Samples are thus quenched in the vacuum system from a known temperature and oxygen pressure. The vacuum system and the low thermal inertia of the filaments provide good conditions for quenching. X-Ray investigations are then made on the quenched filaments; the metallic iridium wire can be used as a

standard for the determination of the X-ray lines.

4. Experimental Results and Discussion

Two kinds of results will be presented below to illustrate various aspects of the method that has been described before. As the first example a very stable oxide, Y_2O_3 , has been chosen. This oxide could be used in the future for various applications as electrodes for MHD conversion because it is a very stable compound with a good emission. In contrast to this, the second kind of data concerned a widely nonstoichiometric oxide which has been studied more: TiO_2 . Each case will be discussed separately.

4.1. Yttrium Oxide

Experimental data of the emission of this oxide have been previously published (10); a more detailed discussion of this system and additional results will be reported here.

4.1.1. Experimental Results

Figure 1 gives a complete set of isotherms. In all the covered range of oxygen pressure J_0 is proportional to $P_{O_2}^{-1/x}$ as expected from Eqs. (3) and (4), with $x \approx 4$. The isobars also yield straight lines (see Fig. 2), whatever the

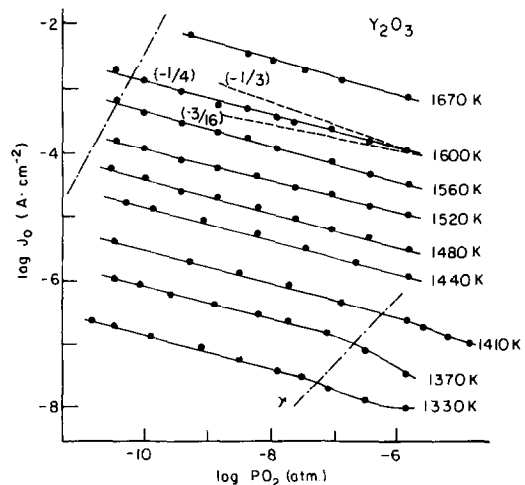


FIG. 1. Thermal emission isotherms for Y_2O_3 .

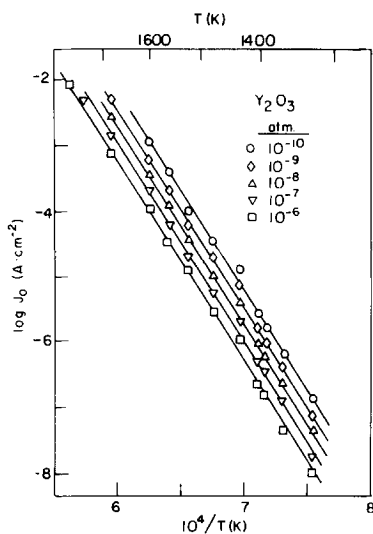


FIG. 2. Thermal emission isobars for Y_2O_3 .

oxygen pressure may be. Indeed the chemisorption of oxygen could modify the electron affinity of the oxide by band bending or dipolar effects (14, 15). But as the chemisorption is an exothermic process any temperature increase would decrease the chemisorbed amount of oxygen and the isobars would not be linear. In this case, as the electron affinity depends on the oxygen pressure, the isobars could not be parallel as observed in Fig. 2. The activation energy of the isobars is $\Phi_R = 6$ eV.

4.1.2. Discussion

4.1.2.1. Comparison of experimental results. There are only a few data available on the nonstoichiometry of pure yttrium oxide. Some authors report the electrical conductivity as a function of the oxygen pressure (9, 16, 17). In the range $1-10^{-6}$ atm, the conductivity increases with the oxygen pressure and a positive sign of the thermoelectric power has been reported (9, 17). However, both these quantities (Eq. (5) for σ_e) depend on the electronic mobility, which is not known. Within that uncertainty the electrical conductivity can give the variations of n and p with the oxygen pressure as long as μ_e and

μ_p are constant with P_{O_2} . For a pure sample and a sufficiently high temperature ($T > 1300$ K) the conduction is electronic (16-18). Agreement is found in the activation energy of the conductivity: $E_{\sigma_e} \approx 1.9 \pm 0.04$ eV as reported by several authors (16, 18-20). In contrast some deviations are found in the slope of the conductivity isotherms:

$$\sigma_p = k_c P_{O_2}^{1/x}, \quad (6)$$

with $x \approx 16/3$ or 6. In some cases (9, 16, 17) the investigated range is too small to offer a valuable distinction. Tallan and Vest (18) have published conductivity data in a very wide range of oxygen pressure. The main characteristic of this report is a minimum of conductivity when plotted versus P_{O_2} ; this minimum was not used in their interpretation. To take it into account their experimental data were fitted according to the theoretical law:

$$\sigma_e = k_n P_{O_2}^{-1/4} + k_p P_{O_2}^{1/4}. \quad (7)$$

The constants when adjusted lead to a good agreement between the calculated curves and the experimental points in range B as can be seen in Fig. 3. In range C Eq. (6) was used with $x = 6$. The slope 3/16 indicated by other authors (see Fig. 3) can be interpreted as an average of the slope in ranges B and C. The calculated values of k_n and k_p are plotted

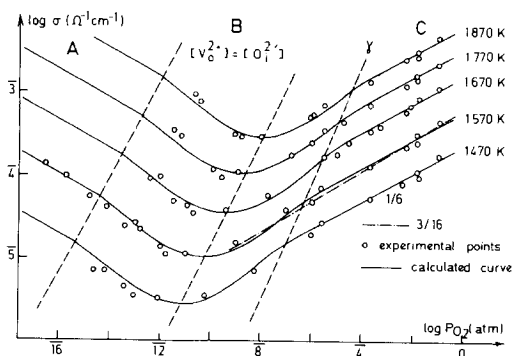


FIG. 3. Electrical conductivity isotherms from Tallan and Vest (18). The calculated curve $\sigma_e = k_n P_{O_2}^{-1/4} + k_p P_{O_2}^{1/4}$ is drawn with a solid line.

versus $1/T$ in Fig. 4a. They are thermally activated as expected.

The contribution of our work is to bring out experimental support for this interpretation, as it is found that J_0 , and then n , varies as $P_{O_2}^{-1/4}$. This is the first direct evidence of such a variation of the electron concentration in the conduction band when the electrical conductivity involves either electrons or holes as is shown by the minimum of σ_e .

4.1.2.2. A model of disorder. One uses the notation of Kroger (6) where $V_O^{2\cdot}$ is a vacancy of oxygen which has lost two electrons and $O_i^{2\cdot}$ denotes an oxygen interstitial with two electrons. The defects can have different degrees of ionization. For a given temperature, if the donor and acceptor concentrations are known, the degree of ionization can be calculated using the various energy levels of ionization (21); unfortunately those levels are generally unknown in oxides. However, with a simple model of two levels (0.03 and 0.2 eV from the conduction band) for the donor, assuming a low compensation of acceptors, it can be shown that above 1273 K the donors are fully ionized (more than 95%) (22). This is typically the case of TiO_2 . For yttrium oxide the levels are not known and at the present time the analysis with fully ionized defects is the best that can be done. Three classical

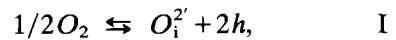
disorders exist: Schottky ($V_Y^{3\cdot}, V_O^{2\cdot}$), cation-Frenkel ($V_Y^{3\cdot}, Y_i^{3\cdot}$), and anion-Frenkel ($O_i^{2\cdot}, V_O^{2\cdot}$). They all give the same dependence for n and p with the oxygen pressure in the range where the electroneutrality equation may be simplified in the atomic defects. An argument in favor of the anion-Frenkel disorder can be found from a crystallographic point of view. First the slightly distorted fluorite structure of Y_2O_3 with one oxygen per four missing (23) with respect to the pure fluorite structure of CaF_2 is certainly adequate to introduce excess oxygen. Second when ZrO_2 , or HfO_2 , is dissolved into Y_2O_3 the density of the compound increases as expected if the excess oxygen is brought into interstitial sites (24, 25). Furthermore this model agrees with the electrical conductivity data in range C where the slope is $1/6$ (Fig. 3). In that range where the holes are the dominating species, the electroneutrality equation

$$p + 2[V_O^{2\cdot}] = n + 2[O_i^{2\cdot}] \quad (8)$$

is simplified in

$$p = 2[O_i^{2\cdot}], \quad (9)$$

where the brackets denote the concentration of the defect. As the creation of an oxygen interstitial is written



the concentration of holes p is calculated using the mass action law for equilibrium I:

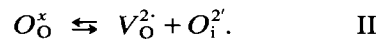
$$[O_i^{2\cdot}]p^2 = k_2P_{O_2}^{1/2}. \quad (10)$$

Using Eq. (9), $p = 2^{1/3}k_2^{1/3}P_{O_2}^{1/6}$ is obtained as expected.

In range B the general Eq. (8) is simplified in:

$$[V_O^{2\cdot}] = [O_i^{2\cdot}] = k_{aF}^{1/2}. \quad (11)$$

k_{aF} is the constant of action mass associated with the equilibrium



As the creation of an oxygen vacancy is

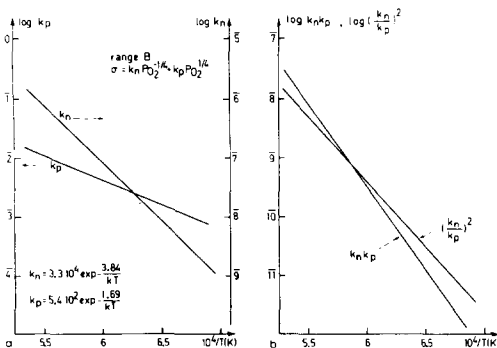
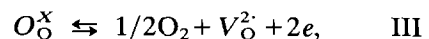


FIG. 4. (a) Variations of the calculated parameters k_n and k_p versus T . (b) Variations of the calculated parameters $k_n k_p$ and $(k_n/k_p)^2$ versus T .

the following equation related to equilibrium III defines k_1 :

$$n^2 [V_{O_2}^{2\cdot}] P_{O_2}^{1/2} = k_1. \quad (12)$$

All these constants, k_1 , k_2 , and k_{aF} , are constants of action mass; they are thus thermally activated with, respectively, energy E_1 , E_2 , and E_{aF} . With Eqs. (11) and (12) and calculating the preexponential term (6):

$$n = \frac{k_1^{\circ 1/2}}{k_{aF}^{\circ 1/4}} T^{3/2} P_{O_2}^{-1/4} \exp\left(-\frac{E_1}{2} - \frac{E_{aF}}{4}\right) / kT, \quad (13)$$

where $k^{\circ 1}$ and k_{aF}° are the preexponential terms of k_1 and k_{aF} . Equation (13) gives the expected dependency which is already observed in thermal emission between n and P_{O_2} . Let us add that partially ionized defects would lead to isotherms with a slope bigger than or nearly equal to $-1/3$ in range B.

4.1.2.3. Evaluation of experimental parameters. Using the anion-Frenkel model with ionized defects which explain correctly the experimental results some constants can be calculated. The energies are all obtained at 0.

—Energy Gap

As the thermal ionization constant $k_i = k_i^{\circ} \exp -E_i/kT$ is given by $k_i = np$, k_i can be calculated using k_n and k_p defined by Eqs. (5) and (7):

$$ne\mu_e = k_n P_{O_2}^{-1/4}, \quad pe\mu_p = k_p P_{O_2}^{1/4}.$$

Thus:

$$k_i = \frac{k_n k_p}{e^2 \mu_e \mu_p}. \quad (14)$$

The variation versus $1/T$ of $k_n k_p$ leads to an estimation of the thermal band gap E_i of Y₂O₃. Such a plot is reported in Fig. 4b; from its slope E_i is found to be ≈ 5.5 eV (relative to 0 K). This is in fair agreement with previous adsorption measurements of light (26). The variations of μ_e and μ_p with the temperature are thus probably small and will be neglected in the following.

—Electron Affinity

The variation of $\log \sigma_e$ versus $1/T$ gives the enthalpic term of k_2 : $E_2 \approx 5.8$ eV when P_{O_2} is in range C of Fig. 3. Using the definitions of k_n and k_p , the ratio k_n/k_p is:

$$k_n/k_p = (k_1/k_2)^{1/2} \mu_e/\mu_p. \quad (15)$$

From Fig. 4b the activation energy of k_n/k_p is evaluated to be ≈ 4.3 eV. Thus from the value of $E_2 = 5.8$ eV, $E_1 = 10.1$ eV is obtained and as

$$k_{aF} = k_1 k_2 / k_i^2,$$

$E_{aF} \approx 4.8$ eV. From Eqs. (3) and (13) the fundamental equation of the thermal emission of electrons can be written in the form:

$$J_0 = \frac{A_0 k_1^{\circ 1/2}}{N_c^0 k_{aF}^{\circ 1/4}} P_{O_2}^{-1/4} T^2 \exp \frac{(E_1/2) - (E_{aF}/4) + \chi}{kT}, \quad (16)$$

where N_c^0 is defined by $N_c = N_c^0 T^{3/2}$. The activation energy of the thermal emission of electrons called Φ_R is thus:

$$\Phi_R = E_1/2 - E_{aF}/4 + \chi. \quad (17)$$

As $\Phi_R \approx 6$ eV, the electron affinity χ is obtained: $\chi \approx 2$ eV. This value is in good agreement with other published data (27). Let us point out that this method is the only one, to our knowledge, for which the oxide is in equilibrium with a known and controlled oxygen partial pressure for the determination of χ .

From the previous constants it is possible to estimate the density of emitted current at the stoichiometry. As $E_i = 5.5$ eV and $\chi = 2$ eV, the work function at the stoichiometry is $\Phi_{St} = 4.75$ eV. Using Eq. (1), at 1570 K $J_{St}^{(1)}$ is obtained: $J_{St}^{(1)} = 2 \times 10^{-7}$ A cm⁻². Assuming $\mu_e = \mu_p$, the minimum of the electrical conductivity gives the oxygen pressure at the stoichiometry: at 1570 K, $P_{O_2} = 10^{-10}$ atm. From Fig. 1, the density of emitted current at this oxygen pressure is $J_{St}^{(2)} = 6 \times 10^{-4}$ A cm⁻². There is thus a big

difference between $J_{St}^{(1)}$ and $J_{St}^{(2)}$; it can be explained as follows.

—First, if the electron mobility is different from the electron hole mobility, the stoichiometry is not observed at the minimum of the electrical conductivity.

—Second, the band gap decreases with the temperature; we have to take this into account in the calculation of the work function at the stoichiometry for 1570 K. With a reduction of 10^{-3} eV K⁻¹, the difference between $J_{St}^{(1)}$ and $J_{St}^{(2)}$ falls to only a factor of 10.

—Third, the effective mass of the electron in the conduction band cannot be neglected. If the vacuum level lies in an allowed energy band, not too close to its edge, a reasonable assumption is to consider the electron which will be emitted, as a free electron. With such an assumption Eq. (3) is written:

$$J_0 = A_0 T^2 \left(\frac{m^*}{m} \right)^{3/2} \exp - \frac{\Phi}{kT}.$$

If $m^* = 10m$ (as, for example, in TiO₂), $J_{St}^{(1)} = 5 \times 10^{-6}$ A cm⁻², only 10 times lower than $J_{St}^{(2)}$.

—Fourth, it has been assumed that the stoichiometry of the surface is the same as that of the bulk when comparison of electron density obtained from emission and conductivity is made. This may be not always true; more quantitative work should be done by doping, for example, to investigate that point.

Thus several points are still in question but it remains that the qualitative agreement is excellent between bulk properties (conductivity) and thermal emission of electrons of Y₂O₃.

4.2. Titanium Dioxide

The results reported here are the first on the thermal emission of electrons for TiO₂, measured as a function of the oxygen pressure. They are divided in two parts: the first part concerns the range 10^{-6} – 10^{-9} atm and 1430–1670 K and will be called “TiO_{2-x}.”

The second part corresponds to higher temperatures where the features are quite different.

4.2.1. Experimental Results

4.2.1.1. TiO_{2-x}. In Fig. 5 are reported the isotherms deduced from isobaric measurements shown in Fig. 6. The data fit straight lines when they are plotted in a log–log scale with a good approximation owing to the procedure. This is true for three orders of magnitude of oxygen pressure. The slopes are:

1430 K	1470 K	1515 K
-1/5.2	-1/4.7	-1/5.1
1560 K	1615 K	1670 K
-1/4.35	-1/4.7	-1/4.1

It is more a fluctuating deviation to a $-1/5$ law than a systematic evolution to a $-1/4$ law which is observed. The values of the thermal emission reported here are measured under an applied potential of 400 V. In this range of potential the log J – $V^{1/2}$ plot is approximately a straight line but its slope is higher than expected, suggesting some contributions of patch effects (28). The true Schottky range would appear at a much higher voltage than 400 V, where other effects, such as field desorption or thermal field emission, could occur (29). In fact the difference between the extrapolated value and the value at 400 V is small as compared to effects discussed later on. Such a high slope for the log J – $V^{1/2}$ plot

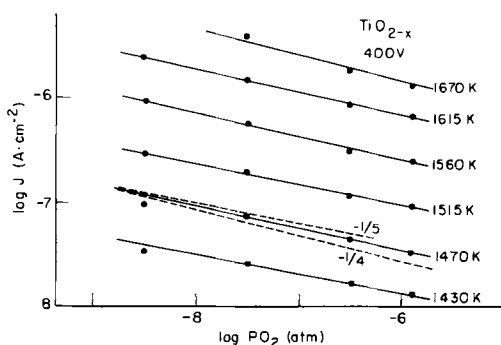


FIG. 5. Thermal emission isotherms for “TiO_{2-x}.”

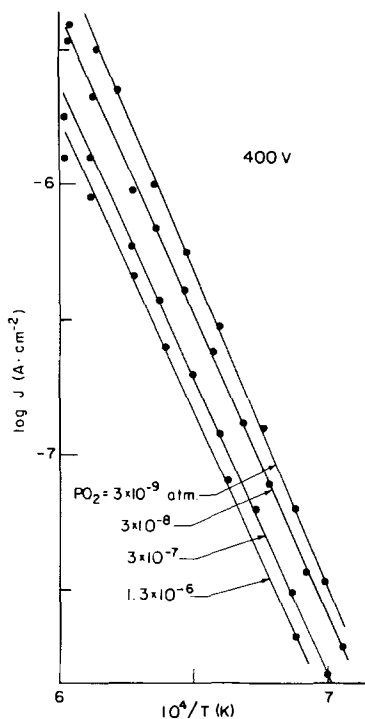


FIG. 6. Thermal emission isobars for " TiO_{2-x} ."

was not found in the case of Y_2O_3 . As can be seen in Fig. 5 the emission of TiO_2 is much lower than the emission of Y_2O_3 , $\times 10^{-3}$, so a higher electron affinity is expected. The measurements are reproducible and reversible as well for isothermic runs as for isobars reported in Fig. 6.

Measurements of the electrical conductivity, made in the vacuum system in the range 1300–1500 K and 10^{-4} – 10^{-8} atm, gave the same dependence as electron emission: the slope was found to be nearly $-1/5$. Figure 7 gives the results of this investigation in a range where the oxygen pressure is difficult to achieve with a buffer gas mixture. The measurements were made with a four-probe method on sintered samples heated in a platinum furnace inside the vacuum chamber. Below 10^{-8} atm the time to obtain the equilibrium was too long, e.g., several hours, to allow reproducible measurements. Under high pressure ($\geq 10^{-6}$ atm) this time is

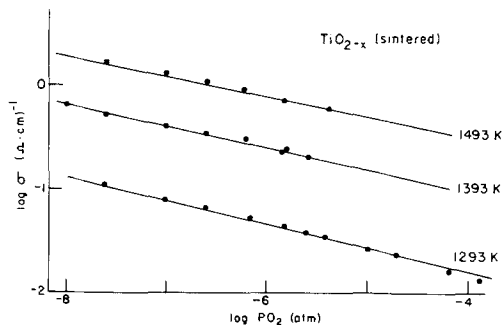


FIG. 7. Electrical conductivity isotherms for " TiO_{2-x} " measured under a low total pressure.

within a scale of minutes. The absolute value of the conductivity agrees well with other published data on the bulk conductivity of this oxide (30).

4.2.1.2. The high-temperature domain. As T is raised at a constant P_{O_2} (for higher T than in Fig. 6) a break occurs in the thermal emission which begins to decrease instead of increasing. The time necessary to reach equilibrium is suddenly multiplied by a factor 50 or 100 (it was in the order of a minute in the domain TiO_{2-x}). After this drop the emission increases again but a hysteresis takes place, preventing a total recovery of the emission to the initial value when the oxide is reoxidized at a low temperature and a high pressure (1300 K and 10^{-5} atm). In any case the difference is low (less than a factor of 2) and is only a memory effect of the high-temperature transformation. In order to plot useful isothermic curves, the

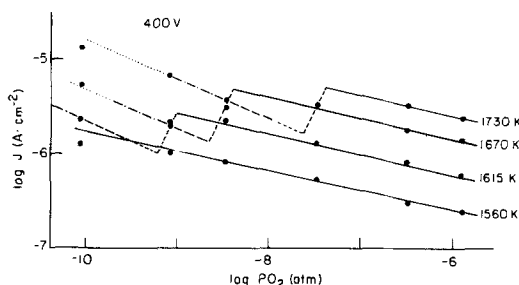


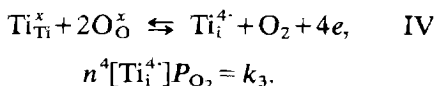
FIG. 8. Thermal emission isotherms for the high-temperature domain of Ti-O compounds. Mixture of phases of Ti_nO_{2n-1} with: ($\cdot \cdot \cdot$) $n = 7$, 8; ($-\cdot -$) $n = 8$, 9; ($---$) $n = 9$, 10; ($---$) $n > 10$.

hysteresis has been corrected by alignment of the points at 1560 K, following the law $J \propto P_{O_2}^{-1/5}$. This is justified by the previous results for the low-temperature range "TiO_{2-x}." Figure 8 is thus obtained; a characteristic drop of the current appears.

X-Ray investigations in this later range were made by quenching the sample in the high-vacuum system as described in Pt. 3. Several samples were quenched at different temperatures and pressures following the isotherms. In the range TiO_{2-x} the crystallographic structure of the rutile is always found. In the pressure range of the drop of the current, the quenched samples are constituted by mixtures of Ti_nO_{2n-1} (31). As the oxygen pressure is decreased the reduction of the oxide increases as shown by the various compounds: n decreases from $n > 10$ (unresolved by X-ray crystallography) to $n = 7$, the more reduced phase observed here. The different phases are indicated in Fig. 8 by several drawings.

4.2.2. Discussion

4.2.2.1. TiO_{2-x}. Using the same argument as in Pt. 4.1, the slope observed in Fig. 5, $-1/5$, is easily explained. The creation of a titanium interstitial is written:



As the electroneutrality equation simplifies as

$$n = 4[Ti_i^{4+}],$$

when the titanium interstitials are the main defects, then

$$n = 4^{1/5} k_3^{1/5} P_{O_2}^{-1/5}. \quad (18)$$

This leads to the law that is approximately observed in emission (Fig. 5). It is noticeable that the same dependence is observed for the bulk conductivity measured under the same conditions of a reduced total pressure containing oxygen only (Fig. 7). This observation and the fact that isobars and isotherms

are straight parallel lines (Fig. 6) rule out any significant exothermic chemisorption effects.

Several experimental papers (30, 32-34) support these results concerning the main defect structure in TiO_{2-x}. There is no doubt that at high temperature (>1273 K) and sufficiently low oxygen pressure ($<10^{-6}$ atm) the main defect is Ti_i⁴⁺. Oxygen vacancies, which would lead to a conductivity variation in $P_{O_2}^{-1/6}$, are probably in a very low concentration.

The ionization degree of Ti_i can be estimated with simple assumptions. If two donor levels are assumed, 0.03 and 0.15-0.20 eV, with a density of states in the conduction band $N_c = 7 \times 10^{21} \text{ cm}^{-3}$ at 1273 K ($m^* = 10m$) and an electron concentration $n = 10^{20} \text{ cm}^{-3}$, the degree of ionization is greater than 95%. Ti_i³⁺ can be neglected under these conditions.

From results published elsewhere (30, 33) a content of 100 ppm of acceptor impurities does not induce any deviations to the $-1/5$ law for $P_{O_2} < 10^{-6}$ atm and $T > 1430$ K. The same observation is found for donor impurities (39). In our case the starting material is a powder with less than 100 ppm impurities (Johnson Matthey), the main impurities being Al (32 ppm) and Fe (16 ppm). They probably evaporate in the vacuum system during the first heating of the filament. It is clear that the vacuum system is more clean than the furnace where the experiments of Baumard and co-workers were made. Thus it seems likely that Ti_i⁴⁺ is present in a high concentration; however, we cannot rule out any contribution of impurities lowering the slope of the isotherms.

Our method using a low total pressure is quite different from the measurements made in a furnace; the agreement is good. Thus heating in a good vacuum system under a known oxygen pressure provides the same results as heating under 1 atm of total pressure. In contrast this is not the case under the so-called vacuum reduction where the sample is heated in the residual gas (35). In

such cases (36) the diffusion coefficients are about 10^5 times smaller than those measured in a buffer gas mixture (37). The conductivity measurements are meaningless in this range because of the absence of equilibrium.

It is interesting to have an idea of the electron affinity of this oxide; however, this is not as simple as in the case of Y_2O_3 . The reason probably arise from an electron affinity varying from place to place on the surface of the polycrystalline sample. It has been shown on metals that the work function is a property sensitive to the indexes of the crystalline face involved (28, 40), and recently changes with the density of steps on the surface of a monocrystal were reported (41). It is then reasonable to assume that a similar property exists for the electron affinity of semiconductors. The spread of the values of the electron affinity affects the measurements of the density of the emitted current (4, 42) and its variations with the temperature. Then it is not possible to calculate directly the electron affinity from the energy of activation Φ_R as previously. However, an unpublished analysis (7) of several results allows one to estimate this mean electron affinity to 4 eV. This is only an order of magnitude in agreement with other unpublished estimations (43). The difference between the various faces of TiO_2 may be as large as 1 eV and could explain the large differences found by various experimenters (4–5.5 eV). This probably reflects the anisotropy of this quadratic compound. In contrast Y_2O_3 has a cubic structure and no such effects were found.

4.2.2.2. *The high-temperature domain.*

The electron emission features are here more complex than in the previous domain: TiO_{2-x} . As reported before the break in the emitted current (Fig. 8) is followed by very long kinetics of equilibration. This suggests a crystallographic reorganization, which has been observed on the quenched samples by X-ray diffraction. In the range where the emission behaves as that of TiO_{2-x} , the

quenched samples always reveals the crystallographic structure of rutile. Otherwise mixtures of the various (44) suboxides Ti_nO_{2n-1} are found. It may be thought that such a transformation may occur during the quenching; however, the existence of stationary compositions has been reported at high temperature by thermogravimetric analysis (45) or electrical conductivity (46). These phases have a very low diffusion coefficient (47) and a hysteresis between reduction and oxidation (45, 46, 48). Such bulk crystallographic reorganizations probably implicate the surface; in fact it has been shown by LEED that reduced monocrystalline TiO_2 has a reconstructed structure (49). The decreases in the current observed in Fig. 8, which seems related to a modification in the electron affinity distribution (4, 7), are due to a surface effect resulting in or initiating the bulk crystallographic reorganization.

The oxygen pressure at the limit of the homogeneity range of TiO_{2-x} is known (32, 46, 50) from measurements in buffer gas mixtures. At 1660 K it lies in the vicinity of 5×10^{-11} atm, thus 100 times lower than the observed value of this experiment. Two hypotheses can be put forward to explain such a difference. At high temperature the sublimation rate is larger than the imposed oxygen rate. As the sublimation is noncongruent the composition of the oxide will change (as Ti_2O_3 is the congruent phase (51)) until a quasi-equilibrium of the rates in and out is reached. From extrapolations of various data on the sublimation of TiO_2 , this is recognized (7) as a possible process for $P_{O_2} \approx 10^{-9} - 10^{-10}$ atm at 1660 K as the total pressure effusing over the Ti–O compounds is in the order of $10^{-9} - 10^{-10}$ atm. In any case a stationary equilibrium is reached as it is observed that the lower the oxygen pressure is the more reduced the sample is. The second hypothesis would be to see the surface reorganization observed here as the initial state of the crystallographic shear process involved in the bulk of the

compound. Such assessment has some experimental and theoretical support (44, 48). Further investigations could clarify this important point.

5. Conclusion

A lot of useful data regarding the nonstoichiometry of Y_2O_3 and TiO_2 have been obtained using the thermal emission of electrons. Two different cases were investigated; one oxide is shown to have a stable cation sublattice, e.g., Y_2O_3 . In contrast to this the other oxide has a stable oxygen sublattice: it is the case of TiO_2 .

The thermal emission of electrons is probably more sensitive to the vicinity of the surface than to the bulk (despite the fact that the escape depth could be quite large as the energy of escape is very low (52)). Then we can conclude from the thermal emission measurements reported here that the involved part of the compound has, at high temperature, the same behavior as the bulk. This unusual technique can bring some new information on the high-temperature properties of the surface vicinity.

Further investigations will attempt to extend the investigated range at higher temperature where the electrical conductivity cannot be presently measured (53).

References

1. G. HERMANN, "The Oxide Coated Cathode," Vol. 2, Chapman and Hall, London (1951).
2. G. A. HAAS, A. SHIH, AND R. E. THOMAS, *Appl. Surface Sci.* **1**, 59 (1977).
3. J. P. LOUP AND A. M. ANTHONY, *Phys. Status Solidi A* **38**, 449 (1970).
4. G. A. HAAS AND R. E. THOMAS, "Techniques of Metal Research," Wiley-Interscience, New York (1972).
5. R. H. HUBE, "Photoconductivity of Solids," Wiley, New York (1967).
6. F. A. KROGER, "The Chemistry of Imperfect Crystal," North-Holland, Amsterdam (1964).
7. P. ODIER, Thesis, Orleans (1977).
8. N. TALLAN, "Electrical Conductivity in Ceramics and Glass," Academic Press, New York (1974).
9. V. J. RUDOLPH, *Z. Naturforsch. A* **14**, 727 (1959).
10. P. ODIER, J. P. LOUP, AND A. M. ANTHONY, *Rev. Int. Hautes Temp. Refract.* **12**, 321 (1971).
11. G. A. HAAS, *J. Appl. Phys.* **28**, 1486 (1957).
12. N. MORGULIS, *Zh. Eksp. Teor. Fiz.* **16**, 959 (1946).
13. J. H. KENNEDY AND A. FOISSY, *J. Electrochem. Soc.* **122**, 482 (1975); R. W. POWERS, *J. Electrochem. Soc.* **122**, 490 (1975).
14. F. G. ALLEN AND G. W. GOBELLI, *Phys. Rev.* **127**, 150 (1962).
15. S. ROY MORRISON, "The Chemical Physics of Surfaces," Plenum, New York (1977).
16. G. ROBERT, Thesis, Grenoble (1967).
17. M. TUSHIHIITO, S. TOMOAKI, AND H. KENZO, *Nippon Daigaku Bensigakubu Shizenkogaku Kenkyusho Kenkyu Kiyo* **10**, 28 (1975).
18. N. TALLAN AND R. W. VEST, *J. Amer. Ceram. Soc.* **49**, 401 (1966).
19. W. NODDACH AND H. WALCH, *Z. Phys. Chem.* **211**, 194 (1959).
20. E. C. SUBBARAO, PH. SUTTER, AND J. HRIZO, *J. Amer. Ceram. Soc.* **48**, 444 (1965).
21. J. S. BLAKEMORE, "Semiconductor Statistics," Pergamon, Oxford (1962).
22. J. F. BAUMARD, Thesis, Orleans (1977).
23. E. LEROY, *U.S. At. Energ. Comm.* **1109**, 26 (1966).
24. D. W. STACY AND D. R. WILDER, *J. Amer. Ceram. Soc.* **58**, 285 (1975).
25. R. BRATTON, *J. Amer. Ceram. Soc.* **52**, 213 (1969).
26. W. H. STREHLOW AND E. L. COOK, *J. Phys. Chem.* **2**, 163 (1973).
27. V. S. FOMENKO, "Handbook of Thermoionic Properties," Plenum, New York (1966); B. S. KUL'VARSKAYA, *Radio Eng. Electron. Phys. (USSR)* **15**, 1471 (1970); H. KAMPZYK AND W. WOLSKI, *Electronica* **2**, 49 (1975); V. V. DANILINA AND Y. A. KOROCHKOV, *Svetotekhnika* **6**, 3 (1973).
28. C. HERRING AND M. H. NICHOLS, *Rev. Mod. Phys.* **21**, 187 (1949).
29. S. G. CHRISTOV, *Surface Sci.* **70**, 32 (1978).
30. J. F. BAUMARD, D. PANIS, AND A. M. ANTHONY, *Rev. Int. Hautes Temp. Refract.* **12**, 321 (1975).
31. S. ANDERSON, B. COLLEN, V. KULENSTIERNA, AND A. MAGNELI, *Acta. Chem. Scand.* **11**, 1641 (1957).
32. C. PICARD AND P. GERDANIAN, *J. Solid State Chem.* **14**, 66 (1975).
33. J. F. BAUMARD AND E. TANI, *Phys. Status Solidi A* **39**, 373 (1977).
34. P. GODE, J. P. PELEGRIN, AND J. J. OEHLIG, *C.R. Acad. Sci. Paris* **28**, 171 (1975).

35. W. D. OHLSEN AND O. W. JOHNSON, *J. Appl. Phys.* **44**, 1927 (1973); J. W. DEFORD AND O. W. JOHNSON, *J. Appl. Phys.* **44**, 3001 (1973); O. W. JOHNSON, J. H. PAKK, AND J. W. DEFORD, *J. Appl. Phys.* **46**, 1026 (1975).
36. E. IGUSHI AND K. YAJIMA, *J. Phys. Soc. Japan* **32**, 1415 (1972).
37. J. F. BAUMARD, *Solid State Commun.* **20**, 859 (1976).
38. P. S. TANNHAUSER, *Solid State Commun.* **1**, 223 (1963).
39. J. F. BAUMARD AND E. TANI, *J. Chem. Phys.* **67**, 857 (1977).
40. R. SMOLUCHOWSKI, *Phys. Rev.* **60**, 661 (1941).
41. B. KRAHAL-URBAN, E. A. NIEKISH, AND H. WAGNER, *Surface Sci.* **64**, 52 (1977); K. BESOCH, B. KRAHAL-URBAN, AND H. WAGNER, *Surface Sci.* **68**, 39 (1977).
42. G. A. HAAS AND R. E. THOMAS, *J. Appl. Phys.* **34**, 3457 (1963); G. A. HAAS AND R. E. THOMAS, *J. Appl. Phys.* **38**, 3969 (1967); G. A. HAAS, H. F. GRAY, AND R. E. THOMAS, *J. Appl. Phys.* **46**, 3293 (1975).
43. O. W. JOHNSON, W. DEFORD, AND S. MYHRA, *J. Appl. Phys.* **43**, 807 (1972).
44. L. A. BURSILL AND B. G. HYDE, in "Progress in Solid State Chemistry (H. Reiss, Ed.), Pergamon, New York (1972).
45. R. R. MERITT, B. G. HYDE, L. A. BURSILL, AND D. K. PHILP, *Phil. Trans. Roy. Soc. London Ser. A* **274**, 627 (1973).
46. J. F. BAUMARD, D. PANIS, AND A. M. ANTHONY, *J. Solid State Chem.* **20**, 43 (1977).
47. J. R. AKSE AND H. B. WHITEHURST, *J. Phys. Chem. Solids* **39**, 457 (1978).
48. J. S. ANDERSON, "Surface and Defect Properties of Solids," The Chemical Society, London (1972).
49. Y. W. CHUNG, W. J. LO, AND G. A. SOMORJAI, *Surface Sci.* **64**, 588 (1977).
50. R. N. BLUMENTHAL AND D. H. WHITMORE, *J. Electrochem. Soc.* **110**, 92 (1963).
51. J. HAMPSON AND P. GILLES, *J. Chem. Phys.* **55**, 3712 (1971).
52. R. B. ANDERSON AND P. T. DAWSON, "Experimental Methods in Catalytic Research," Academic Press, New York (1976).
53. J. C. RIFFLET, P. ODIER, J. P. LOUP, M. HOCH, AND A. M. ANTHONY, *Rev. Int. Hautes Temp. Refract.* **16**, 444, 1979.